First Experimental Study of the Purely Leptonic Decay $D_s^{*+} \to e^+ \nu_e$

M. Ablikim,[1] M. N. Achasov,[13,b] P. Adlarson,[75] R. Aliberti,[36] A. Amoroso,[74a,74c] M. R. An,[40] Q. An,[71,58] Y. Bai,[57] O. Bakina,[37] I. Balossino,[30a] Y. Ban,[47,g] V. Batozskaya,[1,45] K. Begzsuren,[33] N. Berger,[36] M. Berlowski,[45] M. Bertani,[29a] D. Bettoni,[30a] F. Bianchi,[74a,74c] E. Bianco,[74a,74c] J. Bloms,[68] A. Bortone,[74a,74c] I. Boyko,[37] R. A. Briere,[5] A. Brueggemann,[68] H. Cai,[76] X. Cai,[1,58] A. Calcaterra,[29a] G. F. Cao,[1,63] N. Cao,[1,63] S. A. Cetin,[62a] J. F. Chang,[1,58] T. T. Chang,[77] W. L. Chang,[1,63] G. R. Che,[44] G. Chelkov,[37,a] C. Chen,[44] Chao Chen,[55] G. Chen,[1] H. S. Chen,[1,63] M. L. Chen,[1,58,63] S. J. Chen,[43] S. M. Chen,[61] T. Chen,[1,63] X. R. Chen,[32,63] X. T. Chen,[1,63] Y. B. Chen,[1,58] Y. Q. Chen,[35] Z. J. Chen,[26,h] W. S. Cheng,[74c] S. K. Choi,[10] X. Chu,[44] G. Cibinetto,[30a] S. C. Coen,[4] F. Cossio,[74c] J. J. Cui,[50] H. L. Dai,[1,58] J. P. Dai,[79] A. Dbeyssi,[19] R. E. de Boer,[4] D. Dedovich,[37] Z. Y. Deng,[1] A. Denig,[36] I. Denysenko,[37] M. Destefanis,[74a,74c] F. De Mori,[74a,74c] B. Ding,[66,1] X. X. Ding,[47,g] Y. Ding,[41] Y. Ding,[35] J. Dong,[1,58] L. Y. Dong,[1,63] M. Y. Dong,[1,58,63] X. Dong,[76] S. X. Du,[81] Z. H. Duan,[43] P. Egorov,[37,a] Y. L. Fan,[76] J. Fang,[1,58] S. S. Fang,[1,63] W. X. Fang,[1] Y. Fang,[1] R. Farinelli,[30a] L. Fava,[74b,74c] F. Feldbauer,[4] G. Felici,[29a] C. Q. Feng,[71,58] J. H. Feng,[59] K. Fischer,[69] M. Fritsch,[4] C. Fritzsch,[68] C. D. Fu,[1] J. L. Fu,[63] Y. W. Fu,[1] H. Gao,[63] Y. N. Gao,[47,g] Yang Gao,[71,58] S. Garbolino,[74c] I. Garzia,[30a,30b] P. T. Ge,[76] Z. W. Ge,[43] C. Geng,[59] E. M. Gersabeck,[67] A. Gilman,[69] K. Goetzen,[14] L. Gong,[41] W. X. Gong,[1,58] W. Gradl,[36] S. Gramigna,[30a,30b] M. Greco,[74a,74c] M. H. Gu,[1,58] Y. T. Gu,[16] C. Y. Guan,[1,63] Z. L. Guan,[23] A. Q. Guo,[32,63] L. B. Guo,[42] R. P. Guo,[49] Y. P. Guo,[12,f] A. Guskov,[37,a] X. T. Hou,[1,63] T. T. Han,[50] W. Y. Han,[40] X. Q. Hao,[20] F. A. Harris,[65] K. K. He,[55] K. L. He,[1,63] F. H. H. Heinsius,[4] C. H. Heinz,[36] Y. K. Heng,[1,58,63] C. Herold,[60] T. Holtmann,[4] P. C. Hong,[12,f] G. Y. Hou,[1,63] Y. R. Hou,[63] Z. L. Hou,[1] H. M. Hu,[1,63] J. F. Hu,[56,i] T. Hu,[1,58,63] Y. Hu,[1] G. S. Huang,[71,58] K. X. Huang,[59] L. Q. Huang,[32,63] X. T. Huang,[50] Y. P. Huang,[1] T. Hussain,[73] N. Hüsken,[28,36] W. Imoehl,[28] M. Irshad,[71,58] J. Jackson,[28] S. Jaeger,[4] S. Janchiv,[33] J. H. Jeong,[10] Q. Ji,[1] Q. P. Ji,[20] X. B. Ji,[1,63] X. L. Ji,[1,58] Y. Y. Ji,[50] Z. K. Jia,[71,58] P. C. Jiang,[47,g] S. S. Jiang,[40] T. J. Jiang,[17] X. S. Jiang,[1,58,63] Y. Jiang,[63] J. B. Jiao,[50] Z. Jiao,[24] S. Jin,[43] Y. Jin,[66] M. Q. Jing,[1,63] T. Johansson,[75] X. Kui,[1] S. Kabana,[34] N. Kalantar-Nayestanaki,[64] X. L. Kang,[9] X. S. Kang,[41] R. Kappert,[64] M. Kavatsyuk,[64] B. C. Ke,[81] A. Khoukaz,[68] R. Kiuchi,[1] R. Kliemt,[14] L. Koch,[38] O. B. Kolcu,[62a] B. Kopf,[4] M. K. Kuessner,[4] A. Kupsc,[45,75] W. Kühn,[38] J. J. Lane,[67] J. S. Lange,[38] P. Larin,[19] A. Lavania,[27] L. Lavezzi,[74a,74c] T. T. Lei,[71,k] Z. H. Lei,[71,58] H. Leithoff,[36] M. Lellmann,[36] T. Lenz,[36] C. Li,[48] C. Li,[44] C. H. Li,[40] Cheng Li,[71,58] D. M. Li,[81] F. Li,[1,58] G. Li,[1] H. Li,[71,58] H. B. Li,[1,63] H. J. Li,[20] H. N. Li,[56,i] Hui Li,[44] J. R. Li,[61] J. S. Li,[59] J. W. Li,[50] Ke Li,[1] L. J. Li,[1,63] L. K. Li,[1] Lei Li,[3] M. H. Li,[44] P. R. Li,[39,j,k] S. X. Li,[12] T. Li,[50] W. D. Li,[1,63] W. G. Li,[1] X. H. Li,[71,58] X. L. Li,[50] Xiaoyu Li,[1,63] Y. G. Li,[47,g] Z. J. Li,[59] Z. X. Li,[16] Z. Y. Li,[59] C. Liang,[43] H. Liang,[71,58] H. Liang,[35] H. Liang,[1,63] Y. F. Liang,[54] Y. T. Liang,[32,63] G. R. Liao,[15] L. Z. Liao,[50] J. Libby,[27] A. Limphirat,[60] D. X. Lin,[32,63] T. Lin,[1] B. J. Liu,[1] B. X. Liu,[76] C. Liu,[35] C. X. Liu,[1] D. Liu,[19,71] F. H. Liu,[53] Fang Liu,[1] Feng Liu,[6] G. M. Liu,[56,i] H. Liu,[39,j,k] H. B. Liu,[16] H. M. Liu,[1,63] Huanhuan Liu,[1] Huihui Liu,[22] J. B. Liu,[71,58] J. L. Liu,[72] J. Y. Liu,[1,63] K. Liu,[1] K. Y. Liu,[41] Ke Liu,[23] L. Liu,[71,58] L. C. Liu,[44] Lu Liu,[44] M. H. Liu,[12,f] P. L. Liu,[1] Q. Liu,[63] S. B. Liu,[71,58] T. Liu,[12,f] W. K. Liu,[44] W. M. Liu,[71,58] X. Liu,[39,j,k] Y. Liu,[39,j,k] Y. B. Liu,[44] Z. A. Liu,[1,58,63] Z. Q. Liu,[50] X. C. Lou,[1,58,63] F. X. Lu,[59] H. J. Lu,[24] J. G. Lu,[1,58] X. L. Lu,[1] Y. Lu,[7] Y. P. Lu,[1,58] Z. H. Lu,[1,63] C. L. Luo,[42] M. X. Luo,[80] T. Luo,[12,f] X. L. Luo,[1,58] X. R. Lyu,[63] Y. F. Lyu,[44] F. C. Ma,[41] H. L. Ma,[1] J. L. Ma,[1,63] L. L. Ma,[50] M. M. Ma,[1,63] Q. M. Ma,[1] R. Q. Ma,[1,63] R. T. Ma,[63] X. Y. Ma,[1,58] Y. Ma,[47,g] F. E. Maas,[19] M. Maggiora,[74a,74c] S. Maldaner,[4] S. Malde,[69] A. Mangoni,[29b] Y. J. Mao,[47,g] Z. P. Mao,[1] S. Marcello,[74a,74c] Z. X. Meng,[66] J. G. Messchendorp,[14,64] G. Mezzadri,[30a] H. Miao,[1,63] T. J. Min,[43] R. E. Mitchell,[28] X. H. Mo,[1,58,63] N. Yu. Muchnoi,[13,b] Y. Nefedov,[37] F. Nerling,[19,d] I. B. Nikolaev,[13,b] Z. Ning,[1,58] S. Nisar,[11,l] Y. Niu,[50] S. L. Olsen,[63] Q. Ouyang,[1,58,63] S. Pacetti,[29b,29c] X. Pan,[55] Y. Pan,[57] A. Pathak,[35] P. Patteri,[29a] Y. P. Pei,[71,58] M. Pelizaeus,[4] H. P. Peng,[71,58] K. Peters,[14,d] J. L. Ping,[42] R. G. Ping,[1,63] S. Plura,[36] S. Pogodin,[37] V. Prasad,[34] F. Z. Qi,[1] H. Qi,[71,58] H. R. Qi,[61] M. Qi,[43] T. Y. Qi,[12,f] S. Qian,[1,58] W. B. Qian,[63] C. F. Qiao,[63] J. J. Qin,[72] L. Q. Qin,[15] X. P. Qin,[12,f] X. S. Qin,[50] Z. H. Qin,[1,58] J. F. Qiu,[1] S. Q. Qu,[61] C. F. Redmer,[36] K. J. Ren,[40] A. Rivetti,[74c] V. Rodin,[64] M. Rolo,[74c] G. Rong,[1,63] Ch. Rosner,[19] S. N. Ruan,[44] N. Salone,[45] A. Sarantsev,[37,c] Y. Schelhaas,[36] K. Schoenning,[75] M. Scodeggio,[30a,30b] K. Y. Shan,[12,f] W. Shan,[25] X. Y. Shan,[71,58] J. F. Shangguan,[55] L. G. Shao,[1,63] M. Shao,[71,58] C. P. Shen,[12,f] H. F. Shen,[1,63] W. H. Shen,[63] X. Y. Shen,[1,63] B. A. Shi,[63] H. C. Shi,[71,58] J. L. Shi,[12] J. Y. Shi,[1] Q. Q. Shi,[55] R. S. Shi,[1,63] X. Shi,[1,58] J. J. Song,[20] T. Z. Song,[59] W. M. Song,[35,1] Y. J. Song,[12] Y. X. Song,[47,g] S. Sosio,[74a,74c] S. Spataro,[74a,74c] F. Stieler,[36] Y. J. Su,[63] G. B. Sun,[76] G. X. Sun,[1] H. Sun,[63] H. K. Sun,[1] J. F. Sun,[20] K. Sun,[61] L. Sun,[76] S. S. Sun,[1,63] T. Sun,[1,63] W. Y. Sun,[35] Y. Sun,[9] Y. J. Sun,[71,58] Y. Z. Sun,[1] Z. T. Sun,[50] Y. X. Tan,[71,58] C. J. Tang,[54] G. Y. Tang,[1] J. Tang,[59] Y. A. Tang,[76] L. Y. Tao,[72] Q. T. Tao,[26,h] M. Tat,[69] J. X. Teng,[71,58] V. Thoren,[75] W. H. Tian,[52] W. H. Tian,[59] Z. F. Tian,[76] I. Uman,[62b] B. Wang,[1] B. L. Wang,[63] Bo Wang,[71,58] C. W. Wang,[43] D. Y. Wang,[47,g] F. Wang,[72] H. J. Wang,[39,j,k] H. P. Wang,[1,63] K. Wang,[1,58] L. L. Wang,[1] M. Wang,[50] Meng Wang,[1,63] S. Wang,[12,f] S. Wang,[39,j,k] T. Wang,[12,f] T. J. Wang,[44]

W. Wang,[72] W. Wang,[59] W. H. Wang,[76] W. P. Wang,[71,58] X. Wang,[47,g] X. F. Wang,[39,j,k] X. J. Wang,[40] X. L. Wang,[12,f] Y. Wang,[61] Y. D. Wang,[46] Y. F. Wang,[1,58,63] Y. H. Wang,[48] Y. N. Wang,[46] Y. Q. Wang,[1] Yaqian Wang,[18,1] Yi Wang,[61] Z. Wang,[1,58] Z. L. Wang,[72] Z. Y. Wang,[1,63] Ziyi Wang,[63] D. Wei,[70] D. H. Wei,[15] F. Weidner,[68] S. P. Wen,[1] C. W. Wenzel,[4] U. W. Wiedner,[4] G. Wilkinson,[69] M. Wolke,[75] L. Wollenberg,[4] C. Wu,[40] J. F. Wu,[1,63] L. H. Wu,[1] L. J. Wu,[1,63] X. Wu,[12,f] X. H. Wu,[35] Y. Wu,[71] Y. J. Wu,[32] Z. Wu,[1,58] L. Xia,[71,58] X. M. Xian,[40] T. Xiang,[47,g] D. Xiao,[39,j,k] G. Y. Xiao,[43] H. Xiao,[12,f] S. Y. Xiao,[1] Y. L. Xiao,[12,f] Z. J. Xiao,[42] C. Xie,[43] X. H. Xie,[47,g] Y. Xie,[50] Y. G. Xie,[1,58] Y. H. Xie,[6] Z. P. Xie,[71,58] T. Y. Xing,[1,63] C. F. Xu,[1,63] C. J. Xu,[59] G. F. Xu,[1] H. Y. Xu,[66] Q. J. Xu,[17] Q. N. Xu,[31] W. Xu,[1,63] W. L. Xu,[66] X. P. Xu,[55] Y. C. Xu,[78] Z. P. Xu,[43] Z. S. Xu,[63] F. Yan,[12,f] L. Yan,[12,f] W. B. Yan,[71,58] W. C. Yan,[81] X. Q. Yan,[1] H. J. Yang,[51,e] H. L. Yang,[35] H. X. Yang,[1] Tao Yang,[1] Y. Yang,[12,f] Y. F. Yang,[44] Y. X. Yang,[1,63] Yifan Yang,[1,63] Z. W. Yang,[39,j,k] M. Ye,[1,58] M. H. Ye,[8] J. H. Yin,[1] Z. Y. You,[59] B. X. Yu,[1,58,63] C. X. Yu,[44] G. Yu,[1,63] T. Yu,[72] X. D. Yu,[47,g] C. Z. Yuan,[1,63] L. Yuan,[2] S. C. Yuan,[1] X. Q. Yuan,[1] Y. Yuan,[1,63] Z. Y. Yuan,[59] C. X. Yue,[40] A. A. Zafar,[73] F. R. Zeng,[50] X. Zeng,[12,f] Y. Zeng,[26,h] Y. J. Zeng,[1,63] X. Y. Zhai,[35] Y. H. Zhan,[59] A. Q. Zhang,[1,63] B. L. Zhang,[1,63] B. X. Zhang,[1] D. H. Zhang,[44] G. Y. Zhang,[20] H. Zhang,[71] H. H. Zhang,[59] H. H. Zhang,[35] H. Q. Zhang,[1,58,63] H. Y. Zhang,[1,58] J. J. Zhang,[52] J. L. Zhang,[21] J. Q. Zhang,[42] J. W. Zhang,[1,58,63] J. X. Zhang,[39,j,k] J. Y. Zhang,[1] J. Z. Zhang,[1,63] Jianyu Zhang,[63] Jiawei Zhang,[1,63] L. M. Zhang,[61] L. Q. Zhang,[59] Lei Zhang,[43] P. Zhang,[1] Q. Y. Zhang,[40,81] Shuihan Zhang,[1,63] Shulei Zhang,[26,h] X. D. Zhang,[46] X. M. Zhang,[1] X. Y. Zhang,[55] X. Y. Zhang,[50] Y. Zhang,[72] Y. Zhang,[69] Y. T. Zhang,[81] Y. H. Zhang,[1,58] Yan Zhang,[71,58] Yao Zhang,[1] Z. H. Zhang,[1] Z. L. Zhang,[35] Z. Y. Zhang,[44] Z. Y. Zhang,[76] G. Zhao,[1] J. Zhao,[40] J. Y. Zhao,[1,63] J. Z. Zhao,[1,58] Lei Zhao,[71,58] Ling Zhao,[1] M. G. Zhao,[44] S. J. Zhao,[81] Y. B. Zhao,[1,58] Y. X. Zhao,[32,63] Z. G. Zhao,[71,58] A. Zhemchugov,[37,a] B. Zheng,[72] J. P. Zheng,[1,58] W. J. Zheng,[1,63] Y. H. Zheng,[63] B. Zhong,[42] X. Zhong,[59] H. Zhou,[50] L. P. Zhou,[1,63] X. Zhou,[76] X. K. Zhou,[6] X. R. Zhou,[71,58] X. Y. Zhou,[40] Y. Z. Zhou,[12,f] J. Zhu,[44] K. Zhu,[1] K. J. Zhu,[1,58,63] L. Zhu,[35] L. X. Zhu,[63] S. H. Zhu,[70] S. Q. Zhu,[43] T. J. Zhu,[12,f] W. J. Zhu,[12,f] Y. C. Zhu,[71,58] Z. A. Zhu,[1,63] J. H. Zou,[1] and J. Zu[71,58]

(BESIII Collaboration)

[1]*Institute of High Energy Physics, Beijing 100049, People's Republic of China*
[2]*Beihang University, Beijing 100191, People's Republic of China*
[3]*Beijing Institute of Petrochemical Technology, Beijing 102617, People's Republic of China*
[4]*Bochum Ruhr-University, D-44780 Bochum, Germany*
[5]*Carnegie Mellon University, Pittsburgh, Pennsylvania 15213, USA*
[6]*Central China Normal University, Wuhan 430079, People's Republic of China*
[7]*Central South University, Changsha 410083, People's Republic of China*
[8]*China Center of Advanced Science and Technology, Beijing 100190, People's Republic of China*
[9]*China University of Geosciences, Wuhan 430074, People's Republic of China*
[10]*Chung-Ang University, Seoul 06974, Republic of Korea*
[11]*COMSATS University Islamabad, Lahore Campus, Defence Road, Off Raiwind Road, 54000 Lahore, Pakistan*
[12]*Fudan University, Shanghai 200433, People's Republic of China*
[13]*G.I. Budker Institute of Nuclear Physics SB RAS (BINP), Novosibirsk 630090, Russia*
[14]*GSI Helmholtzcentre for Heavy Ion Research GmbH, D-64291 Darmstadt, Germany*
[15]*Guangxi Normal University, Guilin 541004, People's Republic of China*
[16]*Guangxi University, Nanning 530004, People's Republic of China*
[17]*Hangzhou Normal University, Hangzhou 310036, People's Republic of China*
[18]*Hebei University, Baoding 071002, People's Republic of China*
[19]*Helmholtz Institute Mainz, Staudinger Weg 18, D-55099 Mainz, Germany*
[20]*Henan Normal University, Xinxiang 453007, People's Republic of China*
[21]*Henan University, Kaifeng 475004, People's Republic of China*
[22]*Henan University of Science and Technology, Luoyang 471003, People's Republic of China*
[23]*Henan University of Technology, Zhengzhou 450001, People's Republic of China*
[24]*Huangshan College, Huangshan 245000, People's Republic of China*
[25]*Hunan Normal University, Changsha 410081, People's Republic of China*
[26]*Hunan University, Changsha 410082, People's Republic of China*
[27]*Indian Institute of Technology Madras, Chennai 600036, India*
[28]*Indiana University, Bloomington, Indiana 47405, USA*
[29a]*INFN Laboratori Nazionali di Frascati, I-00044 Frascati, Italy*
[29b]*INFN Sezione di Perugia, I-06100 Perugia, Italy*

[29c]University of Perugia, I-06100 Perugia, Italy
[30a]INFN Sezione di Ferrara, I-44122 Ferrara, Italy
[30b]University of Ferrara, I-44122 Ferrara, Italy
[31]Inner Mongolia University, Hohhot 010021, People's Republic of China
[32]Institute of Modern Physics, Lanzhou 730000, People's Republic of China
[33]Institute of Physics and Technology, Peace Avenue 54B, Ulaanbaatar 13330, Mongolia
[34]Instituto de Alta Investigación, Universidad de Tarapacá, Casilla 7D, Arica, Chile
[35]Jilin University, Changchun 130012, People's Republic of China
[36]Johannes Gutenberg University of Mainz, Johann-Joachim-Becher-Weg 45, D-55099 Mainz, Germany
[37]Joint Institute for Nuclear Research, 141980 Dubna, Moscow region, Russia
[38]Justus-Liebig-Universitaet Giessen, II. Physikalisches Institut, Heinrich-Buff-Ring 16, D-35392 Giessen, Germany
[39]Lanzhou University, Lanzhou 730000, People's Republic of China
[40]Liaoning Normal University, Dalian 116029, People's Republic of China
[41]Liaoning University, Shenyang 110036, People's Republic of China
[42]Nanjing Normal University, Nanjing 210023, People's Republic of China
[43]Nanjing University, Nanjing 210093, People's Republic of China
[44]Nankai University, Tianjin 300071, People's Republic of China
[45]National Centre for Nuclear Research, Warsaw 02-093, Poland
[46]North China Electric Power University, Beijing 102206, People's Republic of China
[47]Peking University, Beijing 100871, People's Republic of China
[48]Qufu Normal University, Qufu 273165, People's Republic of China
[49]Shandong Normal University, Jinan 250014, People's Republic of China
[50]Shandong University, Jinan 250100, People's Republic of China
[51]Shanghai Jiao Tong University, Shanghai 200240, People's Republic of China
[52]Shanxi Normal University, Linfen 041004, People's Republic of China
[53]Shanxi University, Taiyuan 030006, People's Republic of China
[54]Sichuan University, Chengdu 610064, People's Republic of China
[55]Soochow University, Suzhou 215006, People's Republic of China
[56]South China Normal University, Guangzhou 510006, People's Republic of China
[57]Southeast University, Nanjing 211100, People's Republic of China
[58]State Key Laboratory of Particle Detection and Electronics, Beijing 100049, Hefei 230026, People's Republic of China
[59]Sun Yat-Sen University, Guangzhou 510275, People's Republic of China
[60]Suranaree University of Technology, University Avenue 111, Nakhon Ratchasima 30000, Thailand
[61]Tsinghua University, Beijing 100084, People's Republic of China
[62a]Near East University, Nicosia, North Cyprus, 99138, Mersin 10, Turkey
[62b]Turkish Accelerator Center Particle Factory Group, Near East University, Nicosia, North Cyprus, 99138, Mersin 10, Turkey
[63]University of Chinese Academy of Sciences, Beijing 100049, People's Republic of China
[64]University of Groningen, NL-9747 AA Groningen, The Netherlands
[65]University of Hawaii, Honolulu, Hawaii 96822, USA
[66]University of Jinan, Jinan 250022, People's Republic of China
[67]University of Manchester, Oxford Road, Manchester M13 9PL, United Kingdom
[68]University of Muenster, Wilhelm-Klemm-Strasse 9, 48149 Muenster, Germany
[69]University of Oxford, Keble Road, Oxford OX13RH, United Kingdom
[70]University of Science and Technology Liaoning, Anshan 114051, People's Republic of China
[71]University of Science and Technology of China, Hefei 230026, People's Republic of China
[72]University of South China, Hengyang 421001, People's Republic of China
[73]University of the Punjab, Lahore-54590, Pakistan
[74a]University of Turin and INFN, University of Turin, I-10125 Turin, Italy
[74b]University of Eastern Piedmont, I-15121 Alessandria, Italy
[74c]INFN, I-10125 Turin, Italy
[75]Uppsala University, Box 516, SE-75120 Uppsala, Sweden
[76]Wuhan University, Wuhan 430072, People's Republic of China
[77]Xinyang Normal University, Xinyang 464000, People's Republic of China
[78]Yantai University, Yantai 264005, People's Republic of China
[79]Yunnan University, Kunming 650500, People's Republic of China
[80]Zhejiang University, Hangzhou 310027, People's Republic of China
[81]Zhengzhou University, Zhengzhou 450001, People's Republic of China

Using 7.33 fb^{-1} of e^+e^- collision data taken with the BESIII detector at the BEPCII collider, we report the first experimental study of the purely leptonic decay $D_s^{*+} \to e^+\nu_e$. Our data contain a signal of this decay with a statistical significance of 2.9σ. The branching fraction of $D_s^{*+} \to e^+\nu_e$ is measured to be $(2.1^{+1.2}_{-0.9\,\text{stat}} \pm 0.2_{\text{syst}}) \times 10^{-5}$, corresponding to an upper limit of 4.0×10^{-5} at the 90% confidence level. Taking the total width of the D_s^{*+} [(0.070 ± 0.028) keV] predicted with the radiative D_s^{*+} decay from the lattice QCD calculation as input, the decay constant of the D_s^{*+} is determined to be $f_{D_s^{*+}} = (214^{+61}_{-46\,\text{stat}} \pm 44_{\text{syst}})$ MeV, corresponding to an upper limit of 354 MeV at the 90% confidence level.

Purely leptonic decays of charmed-strange mesons, $D_s^{(*)+} \to \ell^+\nu_\ell$ ($\ell = e$, μ, or τ), offer the simplest and best-understood probes of the $c \to s$ quark transition [1]. The effects of the strong interaction can be parametrized in terms of the $D_s^{(*)+}$ decay constants ($f_{D_s^{(*)+}}$). Experimental studies of these decays are crucial to test lattice QCD (LQCD) calculations of $f_{D_s^{(*)+}}$ [2–4] and the unitarity of the quark-mixing matrix [5,6]. In addition, the branching fractions (BFs) of $D_s^{(*)+} \to \ell^+\nu_\ell$ for different families of leptons are important to testing lepton flavor universality in the charm sector. Intense experimental investigations [7–11] of the (ground-state) pseudoscalar mesons, e.g., D_s^+, have allowed for precision tests of the standard model (SM). However, for (excited-state) vector mesons, e.g., D_s^{*+}, there have been relatively few theoretical studies, and no experimental study of their weak decays has yet been reported.

Reference [3] states that the $D_s^{*+} \to e^+\nu_e$ decay may be the most promising channel to observe the weak decay of a charmed vector meson. In the SM, the decay width of $D_s^{*+} \to \ell^+\nu_\ell$ can be written as [4]

$$\Gamma(D_s^{*+} \to \ell^+\nu_\ell) = \frac{G_F^2}{12\pi}|V_{cs}|^2 f_{D_s^{*+}}^2 m_{D_s^{*+}}^3 \left(1 - \frac{m_{\ell^+}^2}{m_{D_s^{*+}}^2}\right)^2$$
$$\times \left(1 + \frac{m_{\ell^+}^2}{2m_{D_s^{*+}}^2}\right), \qquad (1)$$

where G_F is the Fermi coupling constant, $|V_{cs}|$ is the $c \to s$ Cabibbo-Kobayashi-Maskawa matrix element, m_{ℓ^+} is the lepton mass, and $m_{D_s^{*+}}$ is the D_s^{*+} mass. The decay constant $f_{D_s^{*+}}$ has been calculated via the nonrelativistic quark model [12–14], the relativistic quark model [14–16], the light-front quark model [17,18], the QCD sum rules [19–21], and the LQCD [4,22–26] with predicted values varying from 212 [12] to 447 [14] MeV. The BF of

$D_s^{*+} \to e^+\nu_e$ is predicted to be from $(0.67 \pm 0.04) \times 10^{-5}$ to $(3.4 \pm 1.4) \times 10^{-5}$ [3,4,27]. The measurement of the BF of $D_s^{*+} \to e^+\nu_e$ is important for testing the predicted BFs by different theories. Using the measured BF of $D_s^{*+} \to e^+\nu_e$, the decay constant $f_{D_s^{*+}}$ can be given by combining with the total decay width of the D_s^{*+} meson ($\Gamma^{\text{total}}_{D_s^{*+}}$) predicted via the radiative D_s^{*+} decay by LQCD. It is crucial to test the predictions based on various methods. Reversely, combining the measured BF of $D_s^{*+} \to e^+\nu_e$, the ratio of $(f_{D_s^{*+}}/f_{D_s^+})$ predicted by LQCD, the D_s^+ lifetime and the BF of the leptonic D_s^+ decay from the particle data group [5] leads to a determination of the unknown $\Gamma^{\text{total}}_{D_s^{*+}}$, which is important for clarifying the large differences in various theoretical predictions of the electromagnetic or strong couplings [3,28–30].

This Letter presents the first experimental search for the decay $D_s^{*+} \to e^+\nu_e$ by using 7.33 fb^{-1} [31] of e^+e^- collision data collected by the BESIII detector at the BEPCII collider at the center-of-mass energies $E_{\text{cm}} = 4.128$, 4.157, 4.178, 4.189, 4.199, 4.209, 4.219, and 4.226 GeV. At these energies, the D_s^{*+} mesons are produced mainly through the process $e^+e^- \to D_s^- D_s^{*+} + c.c.$ In an event where a D_s^- meson is fully reconstructed and comes directly from the e^+e^- collision [called a single-tag (ST) D_s^- meson], the D_s^{*+} meson decaying to $e^+\nu_e$ can be searched for in the recoiling system. Surviving events are called double-tag (DT) events. Throughout this Letter, charge-conjugate modes are always implied.

The charged tracks and photons are selected based on the design and performance [32] of the BESIII detector. The endcap time-of-flight (TOF) system was upgraded with multigap resistive plate chamber technology and now has a time resolution of 60 ps [33,34]. The selection regions for various variables are set as 3 standard deviations of resolution around the nominal peak or via optimization based on figure-of-merit $(S/\sqrt{S+B})$. Monte Carlo (MC) events are generated with a Geant4-based [35] detector simulation software package [36], which includes both the geometrical description and the response of the detector [37]. Inclusive MC samples are produced at the corresponding center-of-mass energies and include all open charm processes, initial state radiation (ISR) production of the $\psi(3770)$, $\psi(3686)$ and J/ψ, and

TABLE I. Requirements for $M_{D_s^-}$ and the obtained values of $N_{ST}^{i\,4.178}$, $\varepsilon_{ST}^{i\,4.178}$, and $\varepsilon_{DT}^{i\,4.178}$ in the ith tag mode at $E_{cm} = 4.178$ GeV, where the uncertainties are statistical only. The differences among the ratios of $\varepsilon_{DT}^{i\,4.178}$ over $\varepsilon_{ST}^{i\,4.178}$ for various modes are mainly due to the M_{rec} and other signal side requirements.

Tag mode	$M_{D_s^-}$ (GeV/c^2)	$N_{ST}^{i\,4.178}$ ($\times 10^3$)	$\varepsilon_{ST}^{i\,4.178}$ (%)	$\varepsilon_{DT}^{i\,4.178}$ (%)
$K^+K^-\pi^-$	[1.950, 1.986]	56.3 ± 0.4	35.67 ± 0.04	24.46 ± 0.11
$K^+K^-\pi^-\pi^0$	[1.947, 1.982]	18.3 ± 0.5	10.62 ± 0.03	8.57 ± 0.07
$\pi^+\pi^-\pi^-$	[1.952, 1.984]	15.8 ± 0.4	46.97 ± 0.14	35.19 ± 0.13
$K_S^0 K^-$	[1.948, 1.991]	14.0 ± 0.2	43.41 ± 0.08	31.71 ± 0.13
$K_S^0 K^-\pi^0$	[1.946, 1.987]	4.9 ± 0.2	15.91 ± 0.09	13.44 ± 0.08
$K^-\pi^+\pi^-$	[1.953, 1.983]	8.2 ± 0.4	40.16 ± 0.22	29.45 ± 0.12
$K_S^0 K_S^0 \pi^-$	[1.951, 1.986]	2.3 ± 0.1	20.82 ± 0.12	14.85 ± 0.09
$K_S^0 K^+\pi^-\pi^-$	[1.953, 1.983]	6.1 ± 0.2	18.11 ± 0.06	13.07 ± 0.08
$K_S^0 K^-\pi^+\pi^-$	[1.958, 1.980]	3.1 ± 0.2	16.12 ± 0.10	12.69 ± 0.08
$\eta_{\gamma\gamma}\pi^-$	[1.930, 2.000]	8.4 ± 0.3	42.61 ± 0.18	34.95 ± 0.13
$\eta_{\pi^+\pi^-\pi^0}\pi^-$	[1.941, 1.990]	2.4 ± 0.1	20.76 ± 0.13	16.87 ± 0.09
$\eta'_{\pi^+\pi^-\eta_{\gamma\gamma}}\pi^-$	[1.940, 1.996]	3.9 ± 0.1	20.48 ± 0.10	16.14 ± 0.09
$\eta'_{\gamma\rho^0}\pi^-$	[1.938, 1.992]	10.7 ± 0.3	29.21 ± 0.12	23.23 ± 0.11
$\eta_{\gamma\gamma}\rho^-$	[1.920, 2.006]	15.3 ± 0.6	16.95 ± 0.09	16.51 ± 0.09
$\eta_{\pi^+\pi^-\pi^0}\rho^-$	[1.927, 1.997]	3.9 ± 0.3	7.52 ± 0.07	7.46 ± 0.06
$\eta_{\gamma\gamma}\pi^+\pi^-\pi^-$	[1.946, 1.990]	9.6 ± 0.7	21.37 ± 0.22	19.99 ± 0.10

$q\bar{q}(q = u, d, s)$ continuum processes, along with Bhabha scattering, $\mu^+\mu^-$, $\tau^+\tau^-$, and $\gamma\gamma$ events. The open charm processes are generated using CONEXC [38]. The effects of ISR [39] and final state radiation (FSR) [40] are considered. The decay modes with known BFs are generated using EVTGEN [41,42] and the other modes are generated using LUNDCHARM [43]. Also, a dedicated "signal MC" sample of $e^+e^- \to D_s^- D_s^{*+} + c.c.$ is generated in which D_s^- is allowed to decay via all possible channels and the D_s^{*+} decays to $e^+\nu_e$.

The ST D_s^- mesons are reconstructed from 16 hadronic decay modes, $D_s^- \to K^+K^-\pi^-$, $K^+K^-\pi^-\pi^0$, $\pi^+\pi^-\pi^-$, $K_S^0 K^-$, $K_S^0 K^-\pi^0$, $K^-\pi^+\pi^-$, $K_S^0 K_S^0 \pi^-$, $K_S^0 K^+\pi^-\pi^-$, $K_S^0 K^-\pi^+\pi^-$, $\eta_{\gamma\gamma}\pi^-$, $\eta_{\pi^+\pi^-\pi^0}\pi^-$, $\eta'_{\pi^+\pi^-\eta_{\gamma\gamma}}\pi^-$, $\eta'_{\gamma\rho^0}\pi^-$, $\eta_{\gamma\gamma}\rho^-$, $\eta_{\pi^+\pi^-\pi^0}\rho^-$, and $\eta_{\gamma\gamma}\pi^+\pi^-\pi^-$, where the subscripts of η (η') represent the decay modes used to reconstruct η (η'). Throughout the text, ρ denotes $\rho(770)$ and $\rho^{-/0}$ decays to $\pi^-\pi^{0/+}$.

All charged tracks except those from K_S^0 must originate from the interaction point with a distance of closest approach less than 1 cm in the transverse plane and less than 10 cm along the z axis. The polar angle θ of each track defined with respect to the symmetry axis of the main drift chamber (MDC) must satisfy $|\cos\theta| < 0.93$. The combined information from the specific ionization energy loss (dE/dx) measured by the MDC, the TOF, and the electromagnetic calorimeter (EMC) are used for particle identification (PID) by forming likelihoods $\mathcal{L}_p$ ($p = K, \pi, e$) for

each particle p hypothesis. Kaon (pion) candidates are required to satisfy $\mathcal{L}_{K(\pi)} > \mathcal{L}_{\pi(K)}$ and $\mathcal{L}_{K(\pi)} > \mathcal{L}_e$.

To select K_S^0 candidates, pairs of oppositely charged tracks with distances of closest approach to the interaction point less than 20 cm along the z axis are assigned as $\pi^+\pi^-$ without PID requirements. These $\pi^+\pi^-$ combinations are required to have an invariant mass within ± 12 MeV/c^2 of the world average K_S^0 mass [5] and have a decay length greater than twice its resolution.

The π^0 and η mesons are reconstructed from photon pairs. Photon candidates are selected from the shower clusters in the EMC. Each electromagnetic shower is required to start within [0, 700] ns from the event start time. The shower energy is required to be greater than 25 (50) MeV in the barrel (endcap) region of the EMC [44]. The opening angle between the candidate shower and the nearest charged track extrapolated to the EMC is required to be greater than 10°. To form π^0 and η candidates, the invariant masses of the selected photon pairs are required to be within the $M_{\gamma\gamma}$ intervals (115,150) and (500, 570) MeV/c^2, respectively. To improve momentum resolution, a kinematic fit is imposed on each chosen photon pair to constrain its invariant mass to the world average π^0 or η mass.

For the tag modes $D_s^- \to \eta_{\pi^0\pi^+\pi^-}\pi^-$ and $\eta_{\pi^0\pi^+\pi^-}\rho^-$, the $\pi^0\pi^+\pi^-$ combinations used to form η candidates are required to be within the intervals (530, 570) MeV/c^2. The η' mesons are reconstructed via two decay modes, $\eta\pi^+\pi^-$ and $\gamma\rho^0$, whose invariant masses are required to be within the intervals (946,970) and (940, 976) MeV/c^2, respectively. In addition, the energy of the γ from $\eta' \to \gamma\rho^0$ decays must be greater than 100 MeV. The ρ^0 and ρ^- candidates are reconstructed from the $\pi^+\pi^-$ and $\pi^-\pi^0$ combinations with invariant masses within the interval (570, 970) MeV/c^2.

To remove soft pions originating from D^* transitions, the momentum of pions directly from the ST D_s^- are required to be greater than 100 MeV/c. For the tag mode $D_s^- \to \pi^+\pi^-\pi^-$ ($D_s^- \to K^-\pi^+\pi^-$), the contribution of the peaking background from the decay $D_s^- \to K_S^0 \pi^-$ ($D_s^- \to K_S^0 K^-$) is rejected by requiring all $\pi^+\pi^-$ combinations to be outside the mass window of (468, 528) MeV/c^2.

In each event, we only keep the ST D_s^- candidate with mass $(M_{D_s^-})$ closest to the world average value per tag mode per charge. Non-$D_s^- D_s^{*+}$ events are further suppressed by requiring that $M_{D_s^-}$ agrees with the world average value within 3σ [5] of each tag mode experimental resolution. The $M_{D_s^-}$ requirements are listed in the second column of Table I. The recoiling mass of the ST D_s^- is defined as

$$M_{rec} \equiv \sqrt{\left(E_{cm} - \sqrt{|\vec{p}_{D_s^-}|^2 c^2 + m_{D_s^-}^2 c^4}\right)^2 / c^4 - |\vec{p}_{D_s^-}|^2 / c^2},$$

(2)

TABLE II. The total ST yields ($N^j_{\rm ST}$) and the averaged signal efficiencies ($\varepsilon^j_{e^+\nu_e}$) for data samples at different energy points, where the uncertainties are statistical only. The differences among the signal efficiencies for different data samples are mainly due to the $M_{\rm rec}$ requirement.

$E_{\rm cm}$ (GeV)	$M_{\rm rec}$ (GeV/c^2)	$N^j_{\rm ST}$ ($\times 10^3$)	$\varepsilon^j_{e^+\nu_e}$ (%)
4.128	[2.105, 2.123]	14.8 ± 0.3	81.31 ± 0.35
4.157	[2.103, 2.127]	22.0 ± 0.5	78.58 ± 0.29
4.178	[2.100, 2.130]	183.1 ± 1.4	77.01 ± 0.16
4.189	[2.100, 2.136]	32.5 ± 0.7	77.25 ± 0.28
4.199	[2.099, 2.140]	30.1 ± 0.9	76.61 ± 0.26
4.209	[2.098, 2.145]	30.9 ± 0.6	74.22 ± 0.24
4.219	[2.098, 2.154]	26.0 ± 0.5	74.49 ± 0.28
4.226	[2.098, 2.167]	41.1 ± 0.7	74.94 ± 0.24

FIG. 1. Fits to the $M_{\rm rec}$ distributions of the ST candidates at $E_{\rm cm} = 4.178$ GeV. Points with error bars are data. Blue solid curves are the fit results. Red dashed curves are the fitted backgrounds. Pairs of red arrows denote the signal regions.

where $(\vec{p}_{\rm cm}, E_{\rm cm})$ is the four momentum of the e^+e^- system and $\vec{p}_{D^-_s}$ is the measured momentum of the ST D^-_s candidate. The $m_{D^-_s}$ is fixed at the world average D^-_s mass. The $M_{\rm rec}$ of the direct D^-_s from an $e^+e^- \to D^-_s D^{*+}_s$ pair tends to form a peak around the world average D^{*+}_s mass, while other processes (e.g., $e^+e^- \to \gamma D^+_s D^-_s$, $e^+e^- \to \pi^0 D^+_s D^-_s$) produce flat distributions. The ST yield for each tag mode is obtained from the fit to the corresponding $M_{\rm rec}$ spectrum. The signal is described by the MC-simulated shape convolved with a Gaussian function representing the resolution difference between data and MC simulation. The nonpeaking background is modeled by a second- or third-order Chebychev polynomial function. The parametrization of the background shape is validated using the inclusive MC sample. Events for the further analysis are selected within the $M_{\rm rec}$ signal regions optimized according to $S/\sqrt{S+B}$, with signal efficiency larger than 90% at each center-of-mass energy. Here, S and B denote the signal and background yields from the inclusive MC samples. The $E_{\rm cm}$-dependent $M_{\rm rec}$ regions are listed in the second column of Table II. As an example, Fig. 1 shows the fit results of the $M_{\rm rec}$ spectra for various tag modes in data at $E_{\rm cm} = 4.178$ GeV. The resulting ST yields ($N^{i\,4.178}_{\rm ST}$), and the corresponding ST efficiencies ($\varepsilon^{i\,4.178}_{\rm ST}$) are summarized in the third and fourth columns of Table I, respectively. The results for $N^{ij}_{\rm ST}$ and $\varepsilon^{ij}_{\rm ST}$ at the other energy points are obtained similarly. The total ST yields $N^j_{\rm ST}$ at various energy points are summarized in the third column of Table II. The i denotes the 16 ST modes, and the j denotes different data samples.

On the recoiling side of the ST D^-_s meson, only one residual charged track is required to be identified as an e^+. The e^+ candidate is required to satisfy $\mathcal{L}_e > 0.8 \times (\mathcal{L}_e + \mathcal{L}_\pi + \mathcal{L}_K)$ and $\mathcal{L}_e > 0.001$. The energy loss of the e^+ candidate due to bremsstrahlung is partially recovered by adding the energies of the EMC showers that are within $10°$ of the e^+ direction and not matched to other particles. The
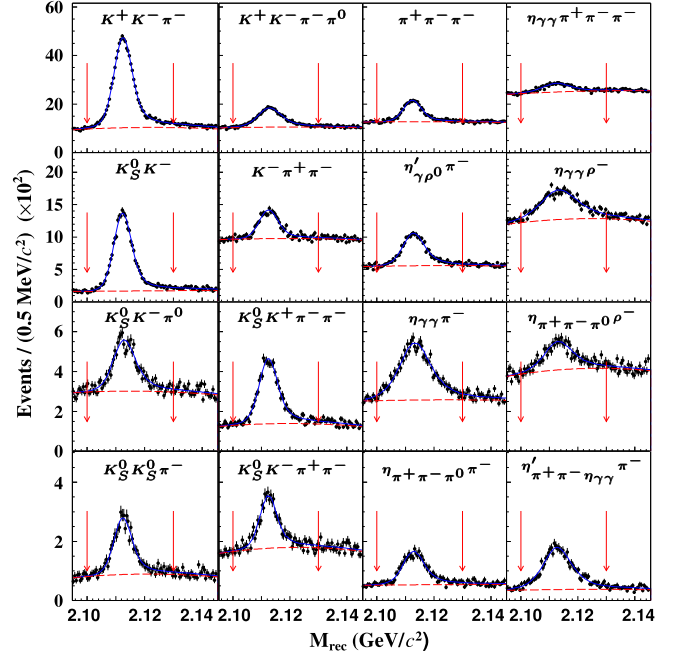
signal is separated from combinatorial backgrounds using the square of the missing mass defined as

$$M^2_{\rm miss} \equiv \left| E_{\rm cm} - \sum_k E_k \right|^2 / c^4 - \left| \sum_k \vec{p}_k \right|^2 / c^2, \quad (3)$$

where E_k and $\vec{p}_k$ are the energy and momentum of particle k in the center-of-mass frame, and the sum runs over the ST D^-_s and the e^+ of the signal side. The measured energy of the e^+ in the rest system of the D^{*+}_s is required to be greater than 1.01 GeV. To suppress backgrounds from hadrons and muons the e^+ candidate is required to have the ratio of the energy deposited in the EMC over the momentum (E/p) within the range [0.8, 1.2]. To suppress background events with extra photon(s), the maximum energy of the unused showers in the DT selection ($E^{\rm max}_{{\rm extra}\gamma}$) is required to be less than 300 MeV. Figure 2 shows the $M^2_{\rm miss}$ distribution for the accepted DT candidate events in data.

To obtain the DT yield, an unbinned maximum extended likelihood fit is performed on the resulting $M^2_{\rm miss}$ distribution. In the fit, the signal and background shapes are obtained from the signal and inclusive MC samples, respectively. The background from the decay $D^+_s \to \tau^+\nu_\tau$ with $\tau^+ \to e^+\nu_e\bar{\nu}_\tau$ tends to form a peak around 0.17 GeV$^2/c^4$ while other backgrounds are flat. All backgrounds from the inclusive MC samples are combined into one background shape. The event yields from the signal and the combined background are free parameters of the fit. The result of the fit to the $M^2_{\rm miss}$ distribution is shown in
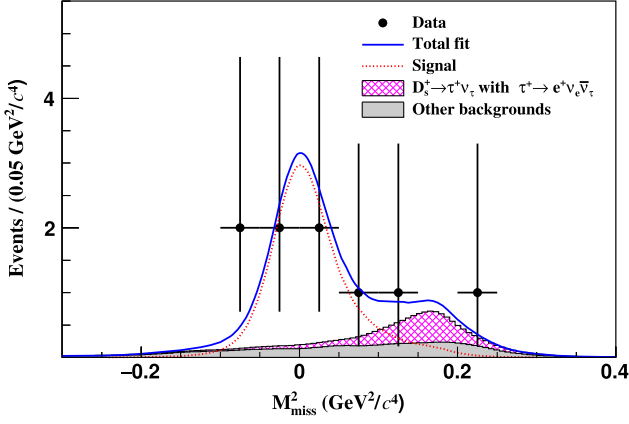
FIG. 2. Fit to the M_{miss}^2 distribution of the $D_s^{*+} \to e^+ \nu_e$ candidates. Points with error bars are data. The blue solid curve is the fit result. The red dotted curve is the signal. The magenta cross-hatched histogram is the decay $D_s^+ \to \tau^+ \nu_\tau$ with $\tau^+ \to e^+ \nu_e \bar{\nu}_\tau$. The gray filled histogram denotes the flat background.

Fig. 2. The obtained signal yield of $D_s^{*+} \to e^+ \nu_e$ is $N_{\text{DT}} = 6.2^{+3.4}_{-2.7}$, where the uncertainty is statistical only. The statistical significance of the signal is 2.9σ, which is estimated by comparing the likelihoods with and without the signal component in the fit and taking into account the number of degrees of freedom.

The efficiencies for reconstructing the DT candidate events are determined with the signal MC sample. The DT efficiencies ($\varepsilon_{\text{DT}}^{i\,4.178}$) obtained at $E_{\text{cm}} = 4.178$ GeV are summarized in the fifth column of Table I. Dividing the DT efficiencies by the ST efficiencies yields the effective efficiencies for detecting $D_s^{*+} \to e^+ \nu_e$. The obtained $\varepsilon_{e^+ \nu_e}^j$ at various energy points are summarized in the fourth column of Table II. The effective signal efficiency for finding $e^+ \nu_e$, weighted by the ST yields for different tag modes and energy points, is obtained to be $\bar{\varepsilon}_{e^+ \nu_e} = (76.63 \pm 0.09)\%$. The BF of $D_s^{*+} \to e^+ \nu_e$ is determined by

$$\mathcal{B}(D_s^{*+} \to e^+ \nu_e) = \frac{N_{\text{DT}}}{\bar{\varepsilon}_{e^+ \nu_e} \sum_j N_{\text{ST}}^j}, \quad (4)$$

to be $(2.1^{+1.2}_{-0.9\,\text{stat}} \pm 0.2_{\text{syst}}) \times 10^{-5}$. The statistical uncertainty is from N_{DT}, and the systematic uncertainty is discussed later.

Because of limited statistics, an upper limit on the BF of $D_s^{*+} \to e^+ \nu_e$ is also set by following Ref. [45] after incorporating the systematic uncertainty via a likelihood scan method. The upper limit of the BF of $D_s^{*+} \to e^+ \nu_e$ is obtained to be 4.0×10^{-5} at the 90% confidence level (C.L.).

The total systematic uncertainty of the BF measurement is determined to be 10.8%. It is obtained by adding in quadrature the individual contributions described below.

The e^+ tracking and PID efficiencies (including the E/p requirement) are studied with radiative Bhabha scattering events. The efficiency differences between data and MC simulation, 0.5% and 1.0%, are assigned as the corresponding systematic uncertainties. The uncertainty in the yield of ST D_s^- mesons is assigned to be 0.9% by examining the relative changes of the fit yields when varying the criteria of truth-matching for signal shape and the order of Chebychev function for background shape. The uncertainty due to the MC statistics is 0.1%. The uncertainty due to the FSR effect is assigned to be 0.5% by studying the radiative Bhabha scattering events [11]. The uncertainty due to different multiplicities of tag environments is assigned as 0.5%.

The efficiency for the requirements of $E_{\text{extra}\,\gamma}^{\text{max}}$ and only one charged track in the signal side is studied with the hadronic DT samples. The systematic uncertainty is taken to be 0.5% considering the efficiency differences between data and MC simulation. For the requirement of the e^+ energy in the rest system of D_s^{*+}, the systematic uncertainty is estimated by changing this requirement by ± 10 MeV. The largest relative change of the BF, 9.5%, is assigned as the corresponding systematic uncertainty.

The systematic uncertainty of the signal shape is estimated by using an alternative MC model and is found to be negligible. The systematic uncertainty in the background shape is examined via two aspects. First, the background shape is replaced with the alternative background shapes obtained by varying the relative fractions of the different background components and shifting the input cross sections by $\pm 1\sigma$. Second, the shape of peaking background is replaced with the one obtained from an $e^+e^- \to D_s^+ D_s^{*-} + c.c$ sample 200 times of the data size, and the combinatorial background shape is replaced with the one derived from the M_{rec} sideband events. The maximum relative change of the BF, 4.8%, is taken as the systematic uncertainty.

With Eq. (1) and the equation (1) of Ref. [10], the total width of the D_s^{*+} is expected to be $\Gamma_{D_s^{*+}}^{\text{total}} = 2.04 \times 10^{-3} \times (f_{D_s^{*+}}/f_{D_s^+})^2 / \mathcal{B}(D_s^{*+} \to e^+ \nu_e)$ eV, after combining the world average values of $\mathcal{B}(D_s^+ \to \mu^+ \nu_\mu)$, the lifetime of the D_s^+, m_e, $m_{D_s^{*+}}$, m_μ, and $m_{D_s^+}$ [5]. Combining with $(f_{D_s^{*+}}/f_{D_s^+}) = 1.12 \pm 0.01$ averaged from LQCD calculations [4,22–26] and $\mathcal{B}(D_s^{*+} \to e^+ \nu_e)$ obtained in this work gives $\Gamma_{D_s^{*+}}^{\text{total}} = (122^{+70}_{-52} \pm 12)$ eV. It agrees with (70 ± 28) eV predicted by LQCD [4] within $\pm 1\sigma$.

Combining our BF measurement with the world average values of G_F, m_e, $m_{D_s^{*+}}$, and $\Gamma_{D_s^{*+}}^{\text{total}}$ given by LQCD [4], we obtain $f_{D_s^{*+}} |V_{cs}| = (208^{+59}_{-45\,\text{stat}} \pm 43_{\text{syst}})$ MeV. Here the second uncertainty is mainly from the systematic uncertainty in the measured $\mathcal{B}(D_s^{*+} \to e^+ \nu_e)$ (10.8%) and the uncertainty in the LQCD predicted $\Gamma_{D_s^{*+}}^{\text{total}}$ (40.0%). Taking $|V_{cs}| = 0.97349 \pm 0.00016$ from the SM global fit [5] as input, we determine $f_{D_s^{*+}} = (214^{+61}_{-46\,\text{stat}} \pm 44_{\text{syst}})$ MeV, corresponding to an upper limit of 354 MeV at the 90% C.L.
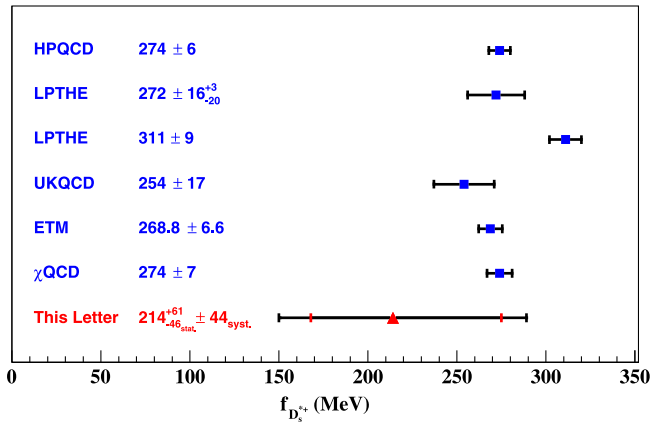
FIG. 3.   Comparison of $f_{D_s^{*+}}$ obtained in this work and LQCD calculations. From top to bottom, the predicted results are from HPQCD [4], LPTHE [22,23], UKQCD [24], ETM [25], and χQCD [26]. For the result of this work, the shorter red error bar denotes the statistical uncertainty only while the longer black error bar combines both statistical and systematic uncertainties.

In summary, by analyzing 7.33 fb^{-1} of e^+e^- collision data collected at $E_{\rm cm}$ from 4.128 to 4.226 GeV with the BESIII detector, we report the first experimental search for the purely leptonic decay $D_s^{*+} \to e^+\nu_e$. The BF of $D_s^{*+} \to e^+\nu_e$ is determined to be $(2.1^{+1.2}_{-0.9\,\rm stat} \pm 0.2_{\rm syst}) \times 10^{-5}$. Our result indirectly constrains the upper limit on the total width $\Gamma^{\rm total}_{D_s^{*+}}$ from the MeV [5] to sub-keV level. Using the $\Gamma_{D_s^{*+}}$ predicted by LQCD and the $|V_{cs}|$ obtained by the global fit in the SM, the decay constant of D_s^{*+} is determined. Figure 3 shows the comparison of the $f_{D_s^{*+}}$ obtained in this work and LQCD calculations. The obtained $f_{D_s^{*+}}$ offers the first experimental test on various theoretical calculations. This analysis opens an avenue to study the weak decays of charmed vector mesons in experiments.

[a]Also at the Moscow Institute of Physics and Technology, Moscow 141700, Russia.
[b]Also at the Novosibirsk State University, Novosibirsk 630090, Russia.
[c]Also at the NRC "Kurchatov Institute," PNPI, 188300 Gatchina, Russia.
[d]Also at Goethe University Frankfurt, 60323 Frankfurt am Main, Germany.
[e]Also at Key Laboratory for Particle Physics, Astrophysics and Cosmology, Ministry of Education; Shanghai Key Laboratory for Particle Physics and Cosmology; Institute of Nuclear and Particle Physics, Shanghai 200240, People's Republic of China.
[f]Also at Key Laboratory of Nuclear Physics and Ion-beam Application (MOE) and Institute of Modern Physics, Fudan University, Shanghai 200443, People's Republic of China.
[g]Also at State Key Laboratory of Nuclear Physics and Technology, Peking University, Beijing 100871, People's Republic of China.
[h]Also at School of Physics and Electronics, Hunan University, Changsha 410082, China.
[i]Also at Guangdong Provincial Key Laboratory of Nuclear Science, Institute of Quantum Matter, South China Normal University, Guangzhou 510006, China.
[j]Also at Frontiers Science Center for Rare Isotopes, Lanzhou University, Lanzhou 730000, People's Republic of China.
[k]Also at Lanzhou Center for Theoretical Physics, Lanzhou University, Lanzhou 730000, People's Republic of China.
[l]Also at the Department of Mathematical Sciences, IBA, Karachi 75270, Pakistan.

[1] H. B. Li and X. R. Lyu, Natl. Sci. Rev. **8**, 11 (2021).
[2] A. Bazavov *et al.* (Fermilab Lattice and MILC Collaborations), Phys. Rev. D **98**, 074512 (2018).

[3] S. Cheng, Y. H. Ju, Q. Qin, and F. S Yu, Eur. Phys. J. C **82,** 1037 (2022).

[4] G. C. Donald, C. T. H. Davies, J. Koponen, and G. P. Lepage (HPQCD Collaboration), Phys. Rev. Lett. **112,** 212002 (2014).

[5] R. L. Workman *et al.* (Particle Data Group), Prog. Theor. Exp. Phys. **2022,** 083C01 (2022).

[6] A. Hocker, H. Lacker, S. Laplace, and F. Le Diberder, Eur. Phys. J. C **21,** 225 (2001).

[7] A. Bazavov *et al.* (Fermilab Lattice and MILC Collaborations), Phys. Rev. D **90,** 074509 (2014).

[8] N. Carrasco *et al.* (ETM Collaboration), Phys. Rev. D **91,** 054507 (2015).

[9] S. Aoki *et al.* (Flavour Lattice Averaging Group), Eur. Phys. J. C **80,** 113 (2020).

[10] M. Ablikim *et al.* (BESIII Collaboration), Phys. Rev. Lett. **122,** 071802 (2019).

[11] M. Ablikim *et al.* (BESIII Collaboration), Phys. Rev. Lett. **127,** 171801 (2021).

[12] M. Abu-Shady and E. M. Khokha, Adv. High Energy Phys. **2018,** 7032041 (2018).

[13] B. H. Yazarloo and H. Mehraban, Eur. Phys. J. Plus **132,** 80 (2017).

[14] D. Ebert, R. N. Faustov, and V. O. Galkin, Phys. Lett. B **635,** 93 (2006).

[15] D. S. Hwang and G. H. Kim, Phys. Rev. D **55,** 6944 (1997).

[16] N. R. Soni and J. N. Pandya, Phys. Rev. D **96,** 016017 (2017).

[17] Q. Chang, X. N. Li, X. Q. Li, F. Su, and Y. D. Yang, Phys. Rev. D **98,** 114018 (2018).

[18] N. Dhiman, H. Dahiya, C. R. Ji, and H. M. Choi, Phys. Rev. D **100,** 014026 (2019).

[19] P. Gelhausen, A. Khodjamirian, A. A. Pivovarov, and D. Rosenthal, Phys. Rev. D **88,** 014015 (2013).

[20] W. Lucha, D. Melikhov, and S. Simula, Phys. Lett. B **735,** 12 (2014).

[21] Z. Wang, Eur. Phys. J. C **75,** 427 (2015).

[22] D. Becirevic, Ph. Boucaud, J. P. Leroy, V. Lubicz, G. Martinelli, F. Mescia, and F. Rapuano, Phys. Rev. D **60,** 074501 (1999).

[23] D. Bečirević, V. Lubicz, F. Sanfilippo, S. Simula, and C. Tarantino, J. High Energy Phys. 02 (2012) 042.

[24] K. Bowler, L. Del Debbio, J. M. Flynn, G. N. Lacagnina, V. I. Lesk, C. M. Maynard, and D. G. Richards (UKQCD Collaboration), Nucl. Phys. **B619,** 507 (2001).

[25] V. Lubicz, A. Melis, and S. Simula (ETM Collaboration), Phys. Rev. D **96,** 034524 (2017).

[26] Y. Chen, W.-F. Chiu, M. Gong, Z. Liu, and Y. Ma (χQCD Collaboration), Chin. Phys. C **45,** 023109 (2021).

[27] Y. L. Yang, Z. L. Li, K. Li, J. S. Huang, and J. F. Sun, Eur. Phys. J. C **81,** 1110 (2021).

[28] B. Pullin and R. Zwicky, J. High Energy Phys. 09 (2021) 023.

[29] H. D. Li, C. D. Lü, C. Wang, Y. M. Wang, and Y. B. Wei, J. High Energy Phys. 04 (2020) 023.

[30] J. L. Goity and W. Roberts, Phys. Rev. D **64,** 094007 (2001).

[31] M. Ablikim *et al.* (BESIII Collaboration), Chin. Phys. C **46,** 113002 (2022).

[32] M. Ablikim *et al.* (BESIII Collaboration), Nucl. Instrum. Methods Phys. Res., Sect. A **614,** 345 (2010).

[33] X. Li *et al.*, Radiat. Detect. Technol. Methods **1,** 13 (2017).

[34] Y. X. Guo *et al.*, Radiat. Detect. Technol. Methods **1,** 15 (2017).

[35] S. Agostinelli *et al.* (Geant4 Collaboration), Nucl. Instrum. Methods Phys. Res., Sect. A **506,** 250 (2003).

[36] Z. Y. Deng *et al.*, Chin. Phys. C **30,** 371 (2006).

[37] K. X. Huang *et al.*, Nucl. Sci. Tech. **33,** 142 (2022).

[38] R. G. Ping, Chin. Phys. C **38,** 083001 (2014).

[39] E. A. Kuraev and Victor S. Fadin, Yad. Fiz. **41,** 733 (1985); [Nucl. Phys. **41,** 466 (1985)].

[40] E. Barberio and Z. Was, Comput. Phys. Commun. **79,** 291 (1994).

[41] D. J. Lange, Nucl. Instrum. Methods Phys. Res., Sect. A **462,** 152 (2001).

[42] R. G. Ping, Chin. Phys. C **32,** 599 (2008).

[43] J. C. Chen, G. S. Huang, X. R. Qi, D. H. Zhang, and Y. S. Zhu, Phys. Rev. D **62,** 034003 (2000); R. L. Yang, R. G. Ping, and H. Chen, Chin. Phys. Lett. **31,** 061301 (2014).

[44] M. Ablikim *et al.* (BESIII Collaboration), Phys. Rev. D **94,** 072004 (2016).

[45] M. Ablikim *et al.* (BESIII Collaboration), Phys. Rev. D **102,** 112005 (2020).